Fisher Matrix Analysis of Velocity-Based Gravitational Lensing

Hunter Martin
Physics Department, UC Berkeley

Dr. David Wittman, Bryant Benson, Matthew Self
Physics Department, UC Davis

The purpose of this project was to conduct a Fisher matrix analysis of a rotational velocity field-based model of a weak gravitational lensing survey. This was to see how well this new model can constrain the lensing parameters, which in turn can help constrain properties of the lensing mass. It was found that this new model can constrain these lensing parameters to a high degree of precision along a single line of sight. Furthermore, the amount of information in a velocity field model was plotted against redshift to determine what redshift, or distance, would provide the most information, an important consideration for selecting good candidate galaxies for measurement. For a lensing mass fixed at a redshift of 0.25, it was found that a source galaxy at a redshift of 0.5 contains the most signal to noise, and would therefore be the site of excellent candidate galaxies for potential measurements using this new model.

I. INTRODUCTION

Gravitational lensing is used as a tool for cosmologists to identify and characterize massive structures in the universe. Since light travels slower in a gravitational potential than in a vacuum, light from a source galaxy bends when passing by a massive object in space, such as a galaxy cluster. This bending causes distortions in the image. Depending on the severity of the distortion, these changes in the image can be classified into two categories: weak gravitational lensing and strong gravitational lensing. Strong gravitational lensing is classified as causing multiple imaging and distorting the images into long arcs, sometimes circles, whereas weak lensing is classified as having minor distortions that merely change the apparent axis ratio of the source galaxy (Bartelmann and Narayan, 1996). See Figure 1 for examples of each. For this project, I was solely concerned with weak gravitational lensing. Weak gravitational lensing can be broken down into two components: shear and convergence. Shear can be broken down further into two other components, the +-component and the x-component of shear, labeled γ_+ and γ_x respectively. Convergence is labeled as κ. Their effects can be best seen on a rotational velocity field, the creation of which is described later, which is shown in Figure 2. γ_+ has an effect of stretching the major or minor axis of the ellipse while compressing the other. γ_x stretches and compresses in the same way as γ_+, but on an axis system 45 degrees from the major and minor axes. κ simply magnifies the image as a whole. An interesting thing to note about γ_x is that it introduces asymmetry into a symmetric velocity field, and de Burgh Day (2015) covers how that asymmetry alone can be used to constrain γ_x. Lensing surveys use the degree of distortion of a background galaxy to determine features of the lensing mass itself, such as its location or mass. The traditional model averages over the images (not the velocity fields) of thousands of background galaxies in a section of the sky to find a bias towards any specific alignment. This works under the assumption that such a bias does not exist in an isotropic universe, and is instead the result of gravitational lensing. In this paper I introduce a new model for the gravitational lensing survey which relies on studying the weak lensing effects on the rotational velocity field of a galaxy. The goal of this project is to perform a Fisher matrix analysis on this new model for weak lensing surveys to see how well implementing this new model can constrain the weak lensing parameters when compared to the traditional weak lensing method.

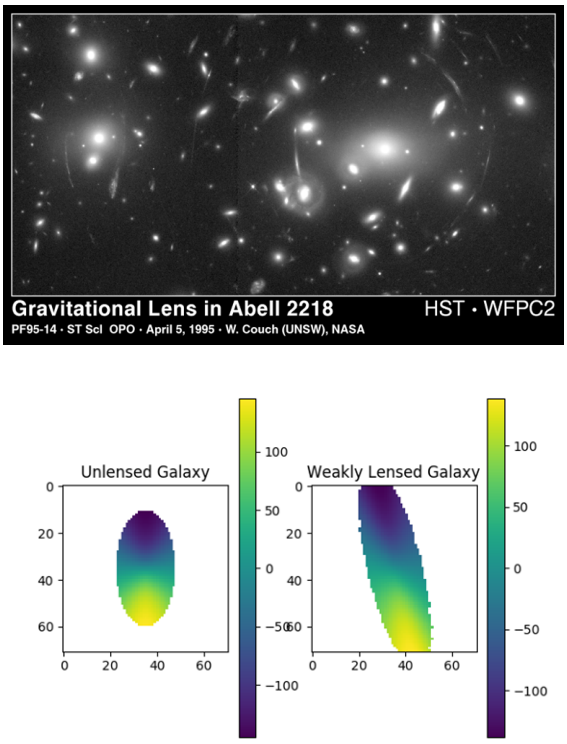

FIG. 1: Here are examples of strong and weak lensing. In the top image, the arc-like streaks are images of strongly lensed galaxies circling around the center of the galaxy cluster. In the bottom image, the lensed galaxy is distorted, but still maintains its elliptical shape.

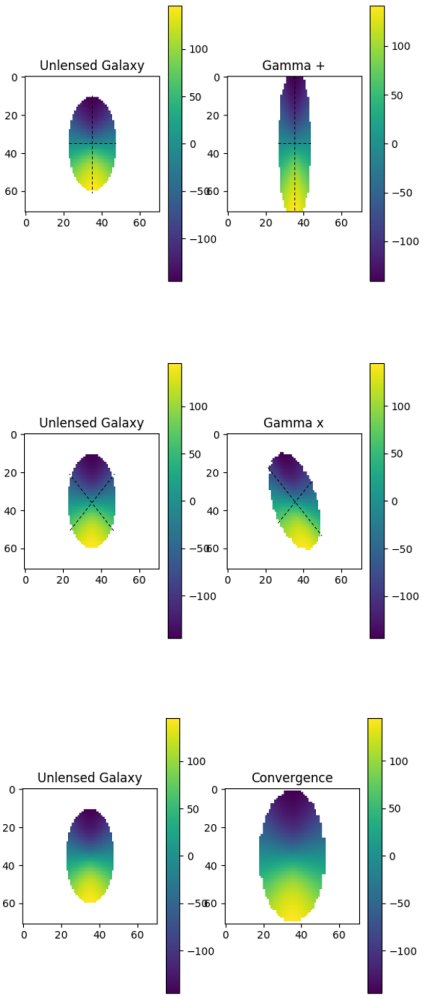

FIG. 2: The effects of the different components of weak lensing are depicted here. The +-component of shear, γ_+, stretches and compresses the major and minor axes, while the cross component of shear, γ_x, stretches and compresses an axis system 45 degrees from the major and minor axes. Convergence, κ, magnifies the image.

II. THEORY

The Fisher matrix is a mathematical tool for calculating the smallest variance achievable in each of the parameters in a given model. When applied to a physical model, the Fisher matrix becomes a powerful tool for designing experiments, as it only relies on a model of the data. This allows for the creation of a sort of metric which a new model can be judged upon before any measurement takes place. As described in D.Wittman (2015), for n model parameters and b observables that relate the parameters, the Fisher matrix is an $n\,x\,n$ matrix with elements:

$$F_{ij} = \sum_b \frac{1}{\sigma_b^2} \frac{\partial f_b}{\partial p_i} \frac{\partial f_b}{\partial p_j}$$

Where σ_b describes the measurement error in each observable. This formula quantifies the amount of information in a model. The use of derivatives in the formula signify that the more prone an observable is to change, the more information it contains, which directly leads to better constrains. This occurs because of a unique property that the Fisher matrix has, which is that its inverse produces the covariance matrix, as seen in Figure 3. A covariance matrix lists the variances of each model parameter along the main diagonal, as well as the covariance between each pair of model parameters on the corresponding off-diagonal element. This information can then be used to understand how well employing a certain model can constrain the parameters of interest. It is important to note here that the Fisher matrix does not provide information on how to take measurements of the model to obtain these constraints, and that the constraints are a result of the information contained within the model itself. For more information on Fisher matrices, see D. Wittman (2015). Because the Fisher

$$\begin{bmatrix} \sigma^2_{p_1} & \sigma_{p_1 p_2} & \sigma_{p_1 p_3} & \cdots & \sigma_{p_1 p_n} \\ \sigma_{p_2 p_1} & \sigma^2_{p_2} & \sigma_{p_2 p_3} & \cdots & \sigma_{p_2 p_n} \\ \sigma_{p_3 p_1} & \sigma_{p_3 p_2} & \sigma^2_{p_3} & \cdots & \sigma_{p_3 p_n} \\ \vdots & & & & \vdots \\ \sigma_{p_n p_1} & \sigma_{p_n p_2} & \sigma_{p_n p_3} & \cdots & \sigma^2_{p_n} \end{bmatrix}$$

FIG. 3: A covariance matrix lists the variances of parameters $p_1 ... p_n$ along the main diagonal, and the covariances between corresponding pairs of parameters on the off-diagonal.

matrix looks at the behavior of the parameters to quantify the amount of information a model contains, it also becomes necessary to include "nuisance" parameters in the model. These parameters have a significant influence on the lensing parameters in question, but provide no insight into the properties of the lensing mass. A good example here is the parameter θ, or the angle of inclination the source galaxy has with respect to the line of sight. Assuming an angle of 0 radians means viewing the galaxy edge-on, the larger the angle, the lesser the amount of velocity is contained in each pixel of the velocity field. However, an angle of 0 radians means that the rotational velocity lies entirely within the line of sight, but contains the minimum number of pixels. This affects the amount of information in the velocity field model because the amount of velocity in a single pixel represents an observable for our Fisher matrix analysis. Therefore, the more velocity per pixel means more information, while at the same time the more pixels means more observables, which further means more information. This tradeoff of information requires θ to be considered in our model. By the same notion, the maximum amount of rotational velocity of the galaxy, v_{max}, must also be considered in the analysis. The last of these "nuisance" parameters is r_0, which represents the radius at which the velocity curve begins to stop increasing rapidly and level out, which has a significant effect on the amount of velocity per pixel. This means that our Fisher matrix analysis models 6 parameters, each of which contributes to the amount of velocity per pixel: γ_+, γ_x, κ, θ, v_{max}, and r_0. Since the Fisher matrix utilizes the

information contained within a specific model, the following question can be asked. What model contains the most information, and would therefore present the tightest constraints on our parameters? The answer in our context depends on the distance, or redshift, of the background galaxy itself. The larger the source redshift, the more distorted the image becomes after passing through the lens, but the smaller the image becomes. The smaller the redshift, and therefore the closer the source is to the lens, the less pronounced the lensing effects are, but the larger the observed size of the image becomes. Furthermore, the amount of information contained within a given model is also dependent on signal to noise, or the ratio of how much of the data is due to the parameters in question versus measurement errors. As an example, while the center of a galaxy is typically well-resolved, the edges of a galaxy are more prone to measurement errors. This signal to noise ratio can then be used as a metric to how much information a model contains with respect to the parameters in question. Therefore, while doing this Fisher matrix analysis, it is also important to consider what models contain the most information, and would therefore make the most suitable candidates for future measurements. In this project I also include an analysis of the relationship between signal to noise and redshift in our results.

III. CONSTRUCTING THE FISHER MATRIX

The bulk of this project was designing a model for velocity field-based weak gravitational lensing surveys, and plugging in the relevant information into the Fisher matrix to see how well this model can constrain its parameters. The first step in doing so was to design a model of the velocity field itself. In our model, I assumed a thin disk galaxy with a symmetrical velocity field. To measure the velocity field of a galaxy, there must be a component of velocity along the line of sight. This allows for the Doppler Effect to create a blueshift and a redshift depending on whether the pixel in consideration has a velocity away or towards the viewer. If the galaxy is viewed face-on, with no component of rotational velocity along the line of sight, then no Doppler Effect can be observed, and the velocity at each pixel would be seen as a constant value across the body of the galaxy. This means that the galaxy itself must be inclined with respect to the line of sight for its velocity field to contain rotational velocity data. Because of this, the 2-dimensional representation of the velocity field appears elliptical, like the one depicted in Figure 4, despite considering a circular galaxy. When calculating the velocity of the galaxy at each pixel, the Universal Rotation Curve (URC) was used to simulate as realistic of a velocity curve as possible (thanks to Bryant Benson for providing the code). Furthermore, the three nuisance parameters, θ, v_{max}, and r_0 were used in constructing the velocity field model.

The next step in the model was to apply the weak lensing effects to the velocity field. As noted previously, these effects can be broken down into three components: the two components of shear (γ_+,γ_-) and convergence (κ). Their effects on the velocity field mapping can be described by the following transformation (De Burgh Day, 2015)

$$\begin{bmatrix} 1-\kappa-\gamma_+ & -\gamma_- \\ -\gamma_- & 1-\kappa-\gamma_+ \end{bmatrix} \quad \begin{bmatrix} x \\ y \end{bmatrix}$$

This transformation was implemented into the Python code by shearing the grid itself, then interpolating the values of each pixel of the original grid onto the sheared grid. After these transformations were applied to the original velocity field, the next step was to begin calculating the Fisher matrix. In order to do this, numerical derivatives had to be calculated for each observable with respect to each parameter. In this model, the observable was the velocity at each pixel, and the parameters were the three lensing parameters and the three nuisance parameters. To calculate the numerical derivative, I wrote Python code to build a velocity field with certain values of the nuisance parameters, then, in the case of the nuisance parameters, build another velocity field with a slightly different value of one of the parameters. In the case of the lensing parameters, I applied the transformation to the original velocity field, then again with a slightly different value of one of the lensing parameters. Taking the difference between the two fields pixel-wise led to the creation of the residual fields, all of which can be seen in Figure 5.

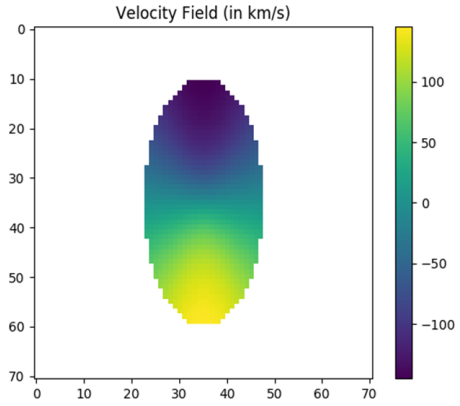

FIG. 4: The modeled symmetric velocity field of a disk galaxy. The top half of the ellipse is traveling towards the observer along the line of sight, while the bottom half is traveling away from the observer along the line of sight.

To make the model more realistic, I implemented a smoothing process to represent the Point Spread Function, since the galaxy itself can be modeled as a point source of light to a telescope. This leads to some measurement error. To model this, I took the residual field from each of the numerical derivatives and applied a Gaussian filter over the field, "smoothing" out the pixel values to create a more continuous velocity field. Afterwards, I divided each smoothed field by the change in the corresponding parameter pixel-wise to obtain the numerical derivative of each pixel of velocity. Then, to further simulate measurement error, I constructed an uncertainty field that was populated by the following function:

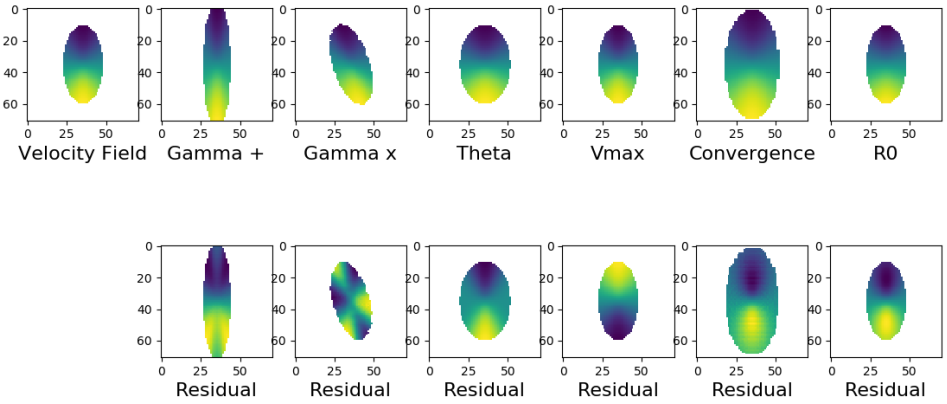

FIG. 5: Lineup of all of the transformations of the velocity field with respect to the different parameters considered in this project. Below is the corresponding residual field when subtracted from a velocity field with a slightly different value of the corresponding parameter. Here, the color blue represents a velocity away from the viewer, and yellow represents a velocity towards a viewer. Green represents lesser values of velocity.

$$\sigma = e^{\frac{3*r}{2*r_{max}}}$$

where r is the distance from the center of the ellipse to a given point, and r_{max} is the distance from the center to the farthest point on the ellipse. The error is described by an exponential function because the center of the galaxy is well-resolved and provides good data, while the edges of the galaxy are less resolved and defined and contain more noise in the data. The derivative fields and the error field were then plugged into the Fisher matrix equation pixel-wise (since each pixel is considered a separate observable), and the resulting matrix was inverted to obtain the covariance matrix.

The second part of the project involved creating the signal to noise versus redshift graph to figure out what candidate galaxies would contain the most information and would therefore be the most suitable candidates for this new model. To accomplish this, the lensing mass was established at redshift 0.25. The source galaxy was then moved back in intervals of 0.1 redshift starting from a redshift of 0.3. At each interval, the Fisher matrix and covariance matrix were calculated to obtain the variance in each of the lensing parameters. The square root of these variances represented the noise in our model. I then calculated the signal by the following formula:

$$signal = \frac{D_{ls}}{D_{diameter}}$$

where D_{ls} is the distance between the lens and the source, and $D_{diameter}$ is the angular diameter distance of the source galaxy. However, distances on the cosmological scale have special circumstances to take into consideration. Since the universe is constantly expanding, distances in one instance of time are different from those in another instance. Cosmologists have worked around this by defining comoving and angular diameter distances. Comoving distances between objects are distances that remain constant if the objects were moving at the same rate the universe is expanding. That is, distances that are measured in the same time. Angular diameter distances, which are used to measure an object's size, are a ratio of the object's transverse size to its angular size, as described by D. Hogg (2000). Since these values are dependent on the redshift of objects relative to each other, and since the redshift from the lensing mass to the source galaxy is unknown, I first had to find D_s and D_l, as shown in Figure 6. To calculate

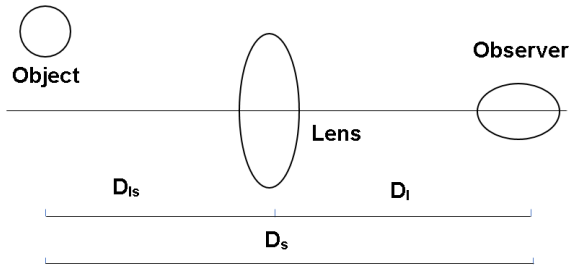

FIG. 6: This is the lens diagram considered in this project. When constructing the signal to noise versus redshift graph, the distance between lens and observer (D_l), the distance between source and observer (D_s), and the distance between lens and source (D_{ls}) are considered.

D_s and D_l, I used the $astropy.comoving\_distance$ function with an $astropy.FlatLambdaCDM$ object. From these val-

ues, I calculated D_{ls} with the following formula (taken from the full formula in Hogg (2000) and simplifying to a flat universe):

$$D_{ls} = \frac{D_s - D_l}{1 + z_s}$$

where z_s represents the redshift of the source galaxy. These distances were calculated for each redshift of the source galaxy, then divided by the angular diameter distance of the source galaxy (calculated using $astropy.angular\_diameter\_distance$) to obtain the signal. The signal was then divided by the noise of each of the three lensing parameters and plotted as a function of redshift.

IV. RESULTS

The covariance matrix obtained from the process outlined above is best depicted graphically. The graph obtained from the covariance matrix is seen in Appendix 1, and is in the form of a corner plot, which is a type of graph that plots a set of parameters with itself pairwise. Within each subplot is a confidence ellipse, which visually depicts the constraint of each parameter, along with the qualitative qualities of the covariance between each parameter. As seen in Figure 7, the width and height of the ellipse depict the constraint of each parameter. As such, all of the ellipses in each row or column have the same height or width, respectively. The angle of the confidence ellipse is also a visual representation of the relationship between those two variables, defined by their covariance. An ellipse that has a positive slope indicates a positive covariance, which means that an increase in one of the parameters would cause a subsequent increase in the other parameter. On the other hand, an ellipse with a negative slope would indicate a negative covariance, meaning that an increase in one of the parameters would cause a subsequent decrease in the other. The histograms along the main diagonal of the corner plot show how one standard deviation of each of the parameters lines up with all of the data. With that being said, the results of the Fisher matrix analysis reveal the following constraints on the lensing parameters using the velocity field model:

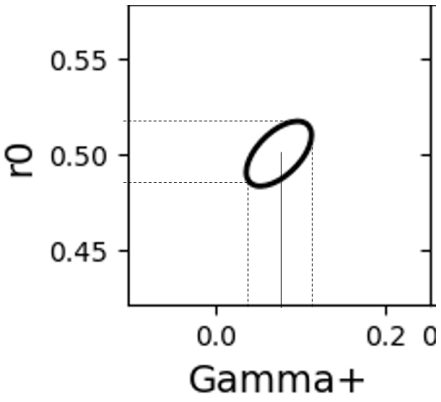

FIG. 7: The r_0 versus γ_+ subplot of the corner plot in Appendix 1 shows an example confidence ellipse. The width of the ellipse shows the constraint on γ_+ if it had a value of 0.075. The height of the ellipse shows the constraint on r_0 if it had a value of 0.5. The angle of the ellipse shows that the two parameters have a positive covariance, meaning that an increase in r_0 would see a subsequent increase in γ_+

Parameter	Actual Value	Constraint
γ_+	0.075	$\pm$ 0.0375
γ_x	0.075	$\pm$ 0.0075
κ	0.1	$\pm$ 0.1

While these constraints are optimistic because the Fisher estimate is the best-case scenario, they do provide a benchmark with which I can compare models. Typical Fisher matrix analyses of traditional photometric methods of lensing surveys reveal that the old model contains enough information to constrain each component of shear to about $\pm$0.2, and contains even less information about convergence. This means that the new velocity field model is $\sim$10x better at constraining these values per galaxy. The traditional method makes up for this by averaging over thousands of galaxies in the night sky. One particularly interesting thing to note here is that the constraint on γ_x is tighter than the γ_+ constraint, while in the old model, they are equivalent. This could be a result of the asymmetry introduced into the symmetrical velocity field by γ_x, which would provide more information, and therefore a better constraint, on γ_x While this new model provides $\sim$10x better constraints per galaxy, it is critical to select good candidate galaxies that provide data equivalent to the model data. As described above, this is best done by looking at the signal to noise versus redshift graph, as pictured in Figure 8. Depicted here is the ratio of signal to noise, or how much information can be separated from measurement error, as a function of the redshift, or how far the source galaxy is from the observer, for all of the weak lensing parameters. As can be seen from the graph, a redshift of about 0.5 (relative to a lens fixed at redshift 0.25) contains the highest ratio of signal to noise for all of the parameters. This means that galaxies at this redshift would have the most information for all of the lensing parameters, meaning that they would be the most suitable candidates for measurement.

V. CONCLUSION

In this project, I conducted a Fisher matrix analysis of a new rotational velocity field model of weak gravitational lensing in order to see how tightly it could constrain the weak lensing parameters, γ_+, γ_x, and κ. The analysis showed that galaxies with this new model can constrain the lensing parameters 10x better than the traditional photometric method. However, since photometric data are cheaper and less time-consuming to take than velocity data, it is important to note that this new model will not serve as a replacement to the standard photometric lensing surveys. Instead, it can serve as a supplementary method to further explore interesting lensing masses and further constrain their properties.

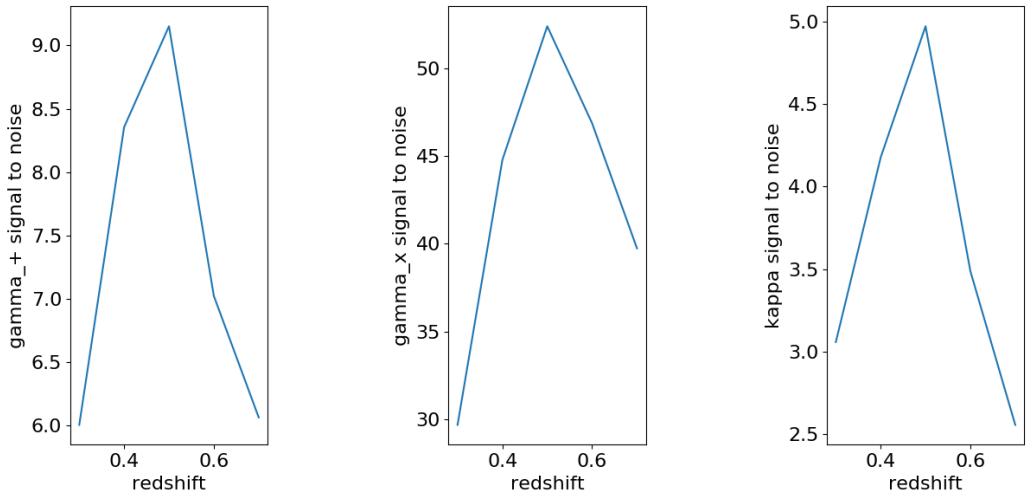

FIG. 8: The signal to noise versus redshift graphs for each of the lensing parameters. All of the three graphs peak at a source galaxy redshift of 0.5 with respect to a lens redshift at 0.25. This means that galaxies at these distances would contain the most information under the velocity field model, and would be suitable candidates for measurements.

Furthermore, I showed that source galaxies with the most information in this new model would occur at a redshift of 0.5 for all of the weak lensing parameters, assuming a fixed lensing mass at redshift 0.25. Since taking velocity data is more expensive and time consuming, this result helps narrow down the field of potential candidate galaxies to ensure that if a measurement is taken, a galaxy with a good signal to noise ratio is chosen.

VI. FUTURE WORK

The future for this project is to continue adding realism to the current model. Current plans are to incorporate information from the photometric field into the model, as proposed by Huff *et al.* (2013). Another plan is to go beyond forecasting the precision, and actually construct the method by which shear and convergence can be inferred.

[1] M. Bartelmann and R. Narayan, "Lectures on Gravitational Lensing," ArXiv Astrophysics e-prints (1996), astro-ph/9606001.
[2] C.O. de Burgh Day, E.N. Taylor, R.L. Webster, and A.M. Hopkins, "Direct Shear Mapping - a new weak lensing tool" *MNRAS* **451**, 2161 (2015), arXiv:1505.06501.
[3] D. Hogg, "Distance measures in cosmology," ArXiv Astrophysics e-prints (2000), arXiv:astro-ph/9905116
[4] D. Wittman, "Fisher Matrix for Beginners," (2015), http://wittman.physics.ucdavis.edu/Fisher-matrix-guide.pdf
[5] E. M. Huff, E. Krause, T. Eifler, M. R. George, and D. Schlegel, ArXiv e-prints (2013), arXiv:1311.1489 [astro-ph.CO]

APPENDIX: 1

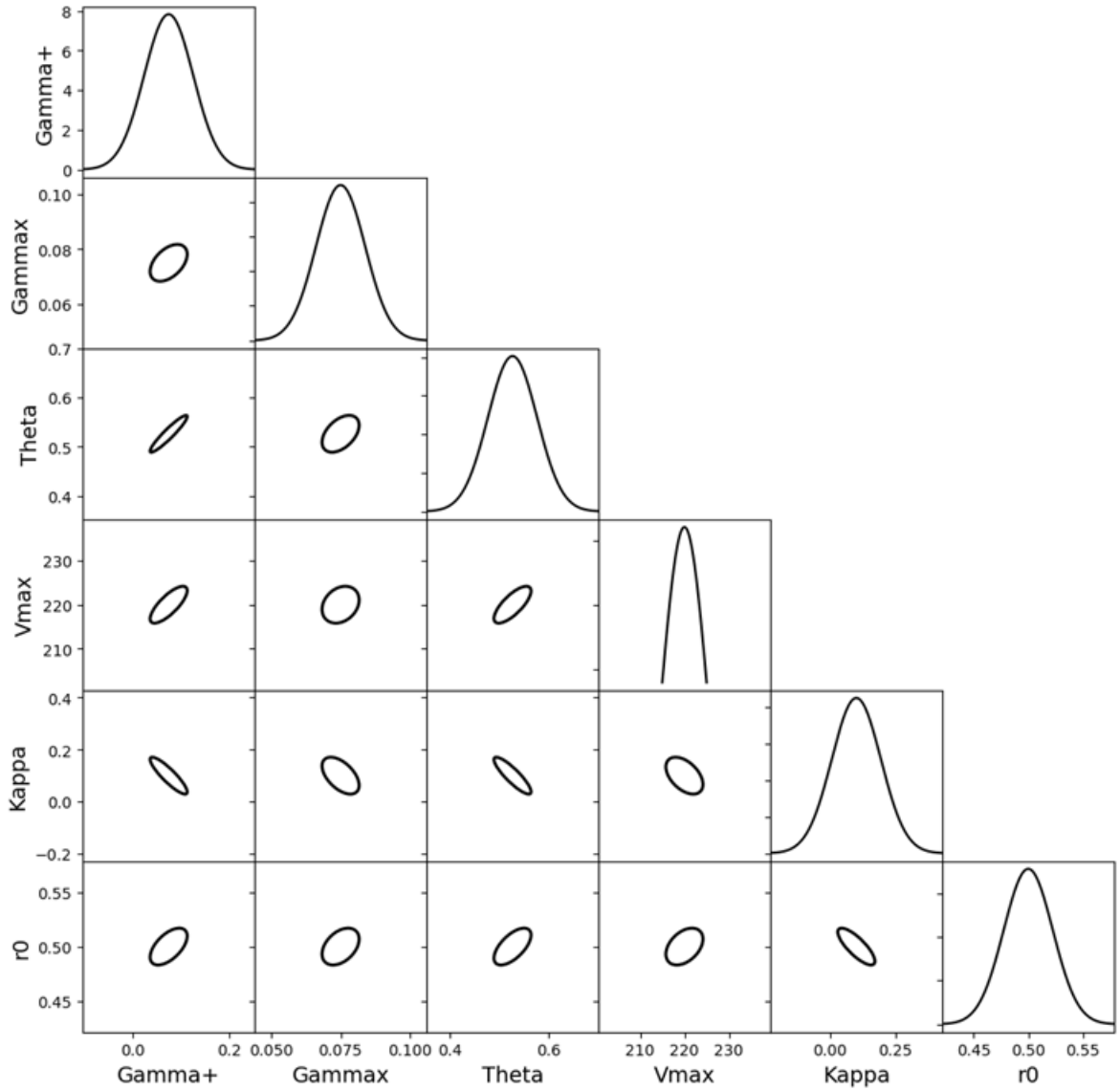

FIG. 9: The corner plot resulting from the Fisher matrix analysis of the rotational velocity field model of weak gravitational lensing.